

# FsNet: Feature Selection Network on High-dimensional Biological Data

Dinesh Singh<sup>1</sup> Makoto Yamada<sup>1,2</sup>  
<sup>1</sup>RIKEN AIP, <sup>2</sup>Kyoto University,

October 21, 2021

## Abstract

Biological data are generally high-dimensional and require efficient machine learning methods that are well generalized and scalable to discover their complex nonlinear patterns. The recent advances in the domain of artificial intelligence and machine learning can be attributed to deep neural networks (DNNs) because they accomplish a variety of tasks in computer vision and natural language processing. However, standard DNNs are not suitable for handling high-dimensional data and data with small number of samples because they require a large pool of computing resources as well as plenty of samples to learn a large number of parameters. In particular, although interpretability is important for high-dimensional biological data such as gene expression data, a nonlinear feature selection algorithm for DNN models has not been fully investigated. In this paper, we propose a novel nonlinear feature selection method called the Feature Selection Network (FsNet), which is a scalable concrete neural network architecture, under high-dimensional and small number of samples setups. Specifically, our network consists of a selector layer that uses a concrete random variable for discrete feature selection and a supervised deep neural network regularized with the reconstruction loss. Because a large number of parameters in the selector and reconstruction layer can easily cause overfitting under a limited number of samples, we use two tiny networks to predict the large virtual weight matrices of the selector and reconstruction layers. The experimental results on several real-world high-dimensional biological datasets demonstrate the efficacy of the proposed approach.

## 1 Introduction

The recent advancements in measuring devices for life sciences have resulted in the generation of massive biological data, which are extremely important for many medical and biological applications, such as disease diagnosis, biomarker discovery, drug development, and forensics [1]. Biological data are substantially high dimensional with a small number of samples and contain complex nonlinear patterns. Machine learning methods are used to discover the complex nonlinear relationships in biological and medical data that are useful in various analytical tasks, such as genome-wide association studies (GWAS) and gene selection [2]. Generally, biological data involve a large number of feature dimensions (e.g.,  $d \geq 10^4$ ) along with a small number of observations (e.g.,  $n \leq 10^3$ ); the most nonlinear learning models are difficult to be trained owing to a large number of model parameters. Hence, the following questions arise naturally: 1) Are all the feature dimensions necessary for building effective models for prediction? 2) What modifications are required in existing machine learning methods to handle such data?

The solution for the first question is selecting the most relevant features that requires a suitable feature selection method [3, 4, 5]. The aim of the feature selection method is to identify a smaller subset of the most relevant features such that it sustains the predictive capability of the data/model while eliminating all other redundant or less relevant features [6, 7, 8]. In feature selection, most of the state-of-the-art methods for computing relevance score are based on either sparse learning methods including Lasso [9] or kernel approaches [10, 11, 6]. These *shallow* approaches work well in practice for biological data. However, the linear models cannot capture biological data due to the nonlinearity in data and

the kernel based approaches heavily depend on the choice of the kernel function. Thus, an arbitrary transformation that is in high correlation with the target variable needs to be trained. A standard approach to learn a nonlinear transformation would be based on deep autoencoders [12]. However, deep autoencoders are useful for computer vision and natural language processing tasks where a large number of training samples are available. In contrast, for high-dimensional biological data where  $n \ll d$ , a good deep model cannot be trained owing to the curse-of-dimensionality. Moreover, they are primarily used for new feature generation instead of feature selection. Training autoencoders for feature selection ultimately result into the discrete optimization objective, i.e., an NP hard problem.

To handle the training of neural networks on high-dimensional data for avoiding overfitting, several approaches were proposed previously. The most widely used approaches are based on random projection with its variants [13, 14]. However, their performance largely depends on the random projection matrix and their usability is limited to dimensionality reduction; therefore, they cannot be applied for feature selection. Another deep learning-based approach employs the concrete autoencoder (CAE) [15], which can select features without supervision using concrete random variables. It should be noted that even though the CAE is an unsupervised model and its performance is poor, it can be extended to incorporate a supervised learning setup. However, we observed that the simple extension is not efficient because the large number of parameters in the CAE can easily lead to overfitting under a limited number of samples (refer to the experimental section for details). In addition, the neurons in its selection layer select a feature independently without knowing the features selected by other neurons; therefore, there is a probability of selecting the same feature more than once, thereby causing redundancy.

To address these issues, we proposed a concrete neural network for nonlinear feature selection (FsNet) on high-dimensional biological data. The FsNet consists of a selector layer that uses concrete random variables [16, 15] for discrete feature selection and a supervised deep neural network regularized with the reconstruction loss. Then, we train the model by maximizing the classification accuracy while minimizing the reconstruction error between the original and reconstructed data from the features selected by the selection layer. Owing to the use of the concrete random variable in the selector layer, we can convert the discrete optimization objective to a continuous optimization objective allowing the back-propagation of gradients using the reparameterization trick. However, due to the large number of parameters in the selector and reconstruction layer, overfitting can easily occur under a limited number of samples. To handle this, we propose the use of two tiny networks to predict the large virtual weight matrices of the selector and reconstruction layers. Consequently, this reduces the size of the model and enables the network to scale ultra high-dimensional datasets on the limited resource device machine. To address the issue of redundancy in feature selection, we apply the softmax functions twice in the selector layer, i.e., during weight prediction (vertically) and concrete variable computation (horizontally), which skews the distribution of the weights and the concrete variable score of a feature toward a single neuron in the selector layer over the epochs. Through experiments on various real-world datasets, we show that the proposed FsNet significantly outperforms the CAE and its supervised counterpart.

## 2 Related Work

To the best of our knowledge, so far, not many research works have used neural networks for nonlinear feature selection for data with high dimensionality and a small number of samples. However, there are several feature selection methods for data with a large number of samples and low dimensionality. Here, we discuss the types of feature selection methods and existing neural network-based feature selection methods along with their drawbacks. We also present the existing approaches that have been made for training a neural network on high-dimensional data. Generally, the feature selection methods are placed into three categories, namely, filter, wrapper, and embedded methods. The filter methods select individual features from a dataset on the basis of various statistical ranking criteria, such as information gain but ignore the interdependence between the features; therefore, they cause redundant feature selection. The wrapper methods can detect the potential relationships between the features because they use sequential search or genetic algorithms to find a subset of features that maximize a given objective function but they are computationally time consuming [17]. The embedded methods incorporate the feature selection task directly into the learning phase of the target machine learning method, such

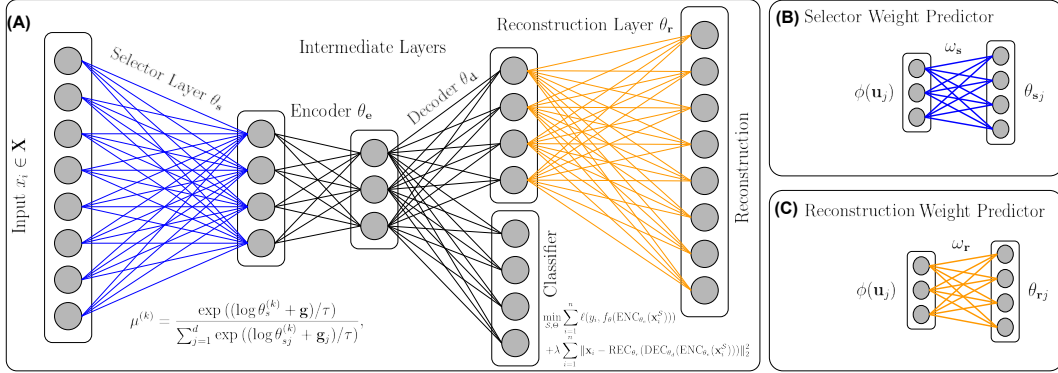


Figure 1: (A) Architecture of FsNet. (B) and (C) are the weight predictor networks for the selector and reconstruction layers, respectively.

as Lasso [9], to select features for the regression problem using  $\ell_1$  regularization.

**Neural network for feature selection:** Researchers have used neural networks for feature selection by adding a regularization term in the loss function or measuring the effect of an input feature on the target variable [18, 19]. Several methods train an additional feature scoring layer that performs elementwise multiplication on the features and the score, and enters them as inputs into the rest of the network [20, 21, 22]. However, they do not select the feature during the training process, which leads to performance degradation after feature selection. The CAE [15] trains an autoencoder with a feature selection layer; however, this method is unsupervised and does not consider the inter-dependency between the features. These methods generally have a significantly large number of parameters in the first layer. Therefore, they cannot be trained for high-dimensional data with a limited number of samples. They work on the assumption that a neural network can undergo generalized training; therefore, they only exhibit good performance for the cases with low-dimensional data (i.e.,  $n \gg d$ ).

**Neural network training on high-dimensional data:** The existing neural network-based methods are computationally infeasible when processing high-dimensional biological data because they suffer from the *curse-of-dimensionality* irrespective of the *regularization constraints*. The biggest drawback of the autoencoders is that they need to store fatty weight matrices of the decoder and encoder. HashedNets [23] addressed the issue by exploiting the inherent redundancy in weights to group them into relatively smaller hash buckets and shared them with all its connections. However, its hash function groups the weights based on their initial values instead of a dynamic grouping, which reduces the options of arbitrary weight learning. Diet-Network [24] used relatively smaller networks to predict the fatty matrices. However, limited to the multilayer perceptron for classification only instead of feature selection. Deep neural pursuit (DNP) [25] selected features from high-dimensional data with a small number of samples based on the changes in the average gradients with multiple dropouts by an individual feature. However, DNP does not consider the reconstruction of the original features or the inter-dependency between the features; thus, the effectiveness and interpretability of the selected features are limited.

These issues make the existing approaches inefficient for processing biological data and raise the need to develop a generalized, interpretable, and scalable method for efficient feature selection from biological data.

### 3 Feature Selection Network (FsNet)

In this section, we formulate the problem first, followed by presenting the architecture and training of the proposed FsNet model for nonlinear feature selection from the high-dimensional data.

### 3.1 Problem Formulation

Let  $\mathbf{X} = (\mathbf{x}_1, \dots, \mathbf{x}_n)^\top = (\mathbf{u}_1, \dots, \mathbf{u}_d) \in \mathbb{R}^{n \times d}$  be the given data matrix where  $\mathbf{x} \in \mathbb{R}^d$  represents the sample vector with  $d$  features and  $\mathbf{u} \in \mathbb{R}^n$  represents the feature vector with  $n$  samples. Let  $\mathbf{y} = (y_1, \dots, y_n)^\top \in \mathbb{R}^n$  be the output/target vector such that  $y_i \in \mathcal{Y}$  represents the output for  $\mathbf{x}_i$ , where  $\mathcal{Y}$  is the domain of the output vector  $\mathbf{y}$ , which is continuous for the regression problems and categorical for the classification problems. We assume that the number of samples are much less than that of the dimensions (i.e.,  $n \ll d$ ).

The final goal of this study is to train a neural network classifier  $f(\cdot) : \mathbb{R}^K \rightarrow \mathcal{Y}$ , which simultaneously identifies a subset  $\mathcal{S} \subseteq \mathcal{F} = \{1, 2 \dots d\}$  of features of specified size  $|\mathcal{S}| = K \ll d$  that can reproduce the remaining  $\mathcal{F} \setminus \mathcal{S}$  features with minimal loss.

### 3.2 Architecture of the FsNet

In this study, we propose the FsNet, where the optimization problem is given by

$$\begin{aligned} \min_{\mathcal{S}, \Theta} \sum_{i=1}^n \ell(y_i, f_{\theta}(\text{ENC}_{\theta_e}(\mathbf{x}_i^{\mathcal{S}}))) \\ + \lambda \sum_{i=1}^n \|\mathbf{x}_i - \text{REC}_{\theta_r}(\text{DEC}_{\theta_d}(\text{ENC}_{\theta_e}(\mathbf{x}_i^{\mathcal{S}})))\|_2^2. \end{aligned} \quad (1)$$

where  $\ell$  is the categorical cross-entropy loss (between the  $f(\mathbf{x}^{\mathcal{S}})$  and  $y$ ),  $\|\cdot\|_2$  is the  $\ell_2$  norm,  $\lambda \geq 0$  is the regularization parameter for the reconstruction loss,  $\Theta$  represents all parameters in the model,  $\text{ENC}(\cdot)$  is the encoder network,  $\text{DEC}(\cdot)$  is the decoder network, and  $\text{REC}(\cdot)$  is the reconstruction layer. As shown in Figure 1(A), the selector and reconstruction layers are the virtual layers and their weights are predicted from the much smaller networks, as shown in Figure 1(B) & (C), respectively. The weight predictor networks are trained on the embedding of the features.

**Selector Layer:** The use of discrete  $\mathcal{S}$  in (1) brakes the propagation of the gradients, thereby making the optimization problem NP-hard, which is difficult to solve. To overcome this difficulty, our selector layer uses a concrete random variable [16] for the continuous relaxation of the discrete one hot vector during the training and computes the gradients using the reparameterization trick. The probability score of the features being selected at the  $k^{\text{th}}$  neuron in the selector layer is defined as

$$\boldsymbol{\mu}^{(k)} = \frac{\exp((\log \boldsymbol{\theta}_s^{(k)} + \mathbf{g})/\tau)}{\sum_{j=1}^d \exp((\log \boldsymbol{\theta}_{s_j}^{(k)} + g_j)/\tau)}, \quad (2)$$

where  $\mathbf{g} \in \mathbb{R}^d$  is drawn from the Gumbel distribution and the temperature  $\tau$  controls the extent of the relaxation.  $\Theta_s = (\boldsymbol{\theta}_{s,1}, \dots, \boldsymbol{\theta}_{s,d}) = (\boldsymbol{\theta}_s^{(1)}, \dots, \boldsymbol{\theta}_s^{(K)})^\top \in \mathbb{R}^{K \times d}$ ,  $\boldsymbol{\theta}_s^{(k)} \in \mathbb{R}_{>0}^K$ ,  $\boldsymbol{\theta}_{s,j} = \boldsymbol{\varphi}_{\omega_s}(\boldsymbol{\phi}(\mathbf{u}_j))$  denotes the virtual weights of the fat selector layer. Here, the feature embedding  $\boldsymbol{\phi}(\mathbf{u}_j)$  for the  $j^{\text{th}}$  feature vector used for training the weight predictor networks is defined as

$$\boldsymbol{\phi}(\mathbf{u}_j) = \boldsymbol{\rho}_j \odot \boldsymbol{\nu}_j, \quad (3)$$

where  $\odot$  denotes the elementwise multiplication while  $\boldsymbol{\rho}_j$  and  $\boldsymbol{\nu}_j$  denote the frequencies and means of the histogram bins of the feature  $\mathbf{u}_j$ , respectively.

Over the epochs,  $\boldsymbol{\mu}^{(k)}$  will converge to a one-hot vector. Because the number of parameters in the selector layer increases with the increase in the size of the input layer  $d$  and the number of neurons  $K$  in the selector layer, it increases the memory requirements for the high-dimensional data and leads to overfitting under a limited number of samples  $n$ . We address both issues by training a tiny weight predictor network  $\boldsymbol{\varphi}_{\omega_s}(\cdot) : \mathbb{R}^b \rightarrow \mathbb{R}_{>0}^K$  to predict the weights connecting the  $j^{\text{th}}$  input element to all  $K$  neurons of the selector layer based on the embedding representation  $\boldsymbol{\phi}(\mathbf{u}_j) \in \mathbb{R}^b$ , where  $b \leq n$

is the size of the embedding representation. Once all the scores  $M = (\mu^{(1)}, \dots, \mu^{(K)}) \in \mathbb{R}^{d \times K}$  are received, the  $K$  best and unique features are selected as

$$\mathcal{S} = \text{uargmax}(M). \quad (4)$$

The function uargmax is defined in Algorithm 1.

---

**Algorithm 1** Unique argmax function uargmax

---

**Input:** matrix  $A \in \mathbb{R}_+^{d \times K}$ , with  $d$  rows and  $K$  cols

**Output:** set of selected indices  $\mathcal{S}$

- 1:  $\mathcal{S} \leftarrow \{\}$
  - 2: **for**  $i = 0 - K$  **do**
  - 3:    $(x, y) \leftarrow$  index of max value in  $A$
  - 4:    $\mathcal{S} \leftarrow \mathcal{S} \cup x$
  - 5:    $A.\text{row}(x) \leftarrow \mathbf{0}$
  - 6:    $A.\text{col}(y) \leftarrow \mathbf{0}$
  - 7: **end for**
  - 8: **return**  $\mathcal{S}$
- 

**Encoder Network:** The goal of the encoder network  $\text{ENC}_{\theta_e}(\cdot) : \mathbb{R}^K \rightarrow \mathbb{R}^h$  is to train a nonlinear hidden representation  $\mathbf{h}$  with  $h$  dimensions from the features  $\mathbf{x}^{\mathcal{S}}$  selected by the selector layer that are suitable for predict the class scores and reconstructing all the features. The hidden representation is defined as

$$\mathbf{h} = \text{ENC}_{\theta_e}(\mathbf{x}^{\mathcal{S}}). \quad (5)$$

**Classifier Network:** The classifier network  $f_{\theta}(\cdot) : \mathbb{R}^h \rightarrow \mathcal{Y}$  predicts the final output form the hidden representation  $\mathbf{h}$  as

$$y = f_{\theta}(\mathbf{h}). \quad (6)$$

**Decoder Network:** Generally, the goal of a decoder function is to reconstruct the original output but the proposed decoder function  $\text{DEC}_{\theta_d}(\cdot) : \mathbb{R}^h \rightarrow \mathbb{R}^{h'}$  computes another hidden representation  $\tilde{\mathbf{h}}$  with  $h'$  dimensions because the last reconstruction layer is defined separately. The decoder function is defined as

$$\tilde{\mathbf{h}} = \text{DEC}_{\theta_d}(\mathbf{h}). \quad (7)$$

**Reconstruction Layer:** The reconstruction layer  $\text{REC}_{\theta_r}(\cdot) : \mathbb{R}^{h'} \rightarrow \mathbb{R}^d$  computes the original output  $\hat{\mathbf{x}}$  as a linear combination of the hidden representation  $\tilde{\mathbf{h}}$  from the decoder network as follows:

$$\hat{\mathbf{x}} = \text{REC}_{\theta_r}(\tilde{\mathbf{h}}), \quad (8)$$

where  $\theta_r^{(j)} = \varphi_{\omega_r}(\phi(\mathbf{u}_j))$  denotes the virtual weights of the  $j^{\text{th}}$  neuron in the reconstruction layer. Similar to the selector layer,  $\varphi_{\omega_r}(\cdot) : \mathbb{R}^b \rightarrow \mathbb{R}^{h'}$  is trained on  $\phi(\mathbf{u}_j)$  to predict the weights connecting the  $j^{\text{th}}$  neuron of the reconstruction layer to all  $h'$  neurons of the last layer of the decoder network. The *pseudocode* for FsNet training is given in Algorithm 2.

## 4 Empirical Evaluation

In this section, we present the experiments conducted to compare the performance of the proposed FsNet to the existing approaches on standard datasets. The objective of the experiments is to demonstrate the efficiency and effectiveness of

---

**Algorithm 2** Training of FsNet

---

**Input:** data matrix  $\mathbf{X} \in \mathbb{R}^{n \times d}$ , output labels  $y \in \{1, \dots, L\}$ ,  $K$  target number of features, encoder network  $\text{ENC}_{\theta_e}(\cdot)$ , decoder network  $\text{DEC}_{\theta_d}(\cdot)$ , reconstruction function  $\text{REC}_{\theta_r}(\cdot)$ , classification network  $f_{\theta}(\cdot)$ , weight prediction networks  $\varphi_{\omega_s}(\cdot)$  &  $\varphi_{\omega_r}(\cdot)$ , learning rate  $\eta$ , start temperature  $\tau_0$ , end temperature  $\tau_E$ , and number of epochs  $E$

**Output:** set of selected features  $\mathcal{S}$ , model parameters  $\Theta$

- 1: Initialize  $\Theta = \{\omega_s, \theta_e, \theta_d, \omega_r, \theta\}$ .
  - 2: **for**  $e \in \{1, \dots, E\}$  **do**
  - 3:   Update the temperature  $\tau = \tau_0(\tau_E/\tau_0)^{e/E}$
  - 4:    $(\theta_{s,1}, \dots, \theta_{s,d}) \leftarrow (\varphi_{\omega_s}(\phi(\mathbf{u}_1)) \cdots \varphi_{\omega_s}(\phi(\mathbf{u}_d)))$
  - 5:    $\boldsymbol{\mu}^{(k)} \leftarrow \text{Concrete}(\theta_s^{(k)}, \tau)$  using (2)
  - 6:    $\mathbf{M} \leftarrow (\boldsymbol{\mu}^{(1)}, \dots, \boldsymbol{\mu}^{(K)})$
  - 7:    $\mathcal{S} \leftarrow \text{uargmax}(\mathbf{M})$
  - 8:    $\mathbf{h} \leftarrow \begin{cases} \text{ENC}_{\theta_e}(\mathbf{M}^\top \mathbf{x}_i) & \text{if training,} \\ \text{ENC}_{\theta_e}(\mathbf{x}^{\mathcal{S}}) & \text{otherwise} \end{cases}$
  - 9:    $\hat{y} \leftarrow f_{\theta}(\mathbf{h})$
  - 10:    $\tilde{\mathbf{h}} \leftarrow \text{DEC}_{\theta_d}(\mathbf{h})$
  - 11:    $(\theta_r^{(1)}, \dots, \theta_r^{(d)}) \leftarrow (\varphi_{\omega_r}(\phi(\mathbf{u}_1)) \cdots \varphi_{\omega_r}(\phi(\mathbf{u}_d)))$
  - 12:    $\hat{\mathbf{x}} \leftarrow \text{REC}_{\theta_r}(\tilde{\mathbf{h}})$
  - 13:   Define the loss  $L$ .
  - 14:   Compute  $\nabla_{\omega_r} L, \nabla_{\theta} L, \nabla_{\theta_d} L$ , and  $\nabla_{\theta_e} L$  using backpropagation.
  - 15:   Compute  $\nabla_{\omega_s^{(k)}} L$  using reparameterization trick
  - 16:   Update  $\omega_r \leftarrow \omega_r - \eta \nabla_{\omega_r} L$ ,  $\theta \leftarrow \theta - \eta \nabla_{\theta} L$ ,  
           $\theta_d \leftarrow \theta_d - \eta \nabla_{\theta_d} L$ ,  $\theta_e \leftarrow \theta_e - \eta \nabla_{\theta_e} L$ , and  
           $\omega_r^{(k)} \leftarrow \omega_r^{(k)} - \eta \nabla_{\omega_r^{(k)}} L$
  - 17: **end for**
  - 18: **return**  $\mathcal{S}, \Theta$
- 

the proposed FsNet in feature selection for high-dimensional datasets in comparison to the existing approaches instead of improving the *state-of-the-art* methods on a particular dataset. Therefore, we conducted the experiments on all datasets with a fixed architecture, defined as  $[d \rightarrow K \rightarrow 64 \rightarrow 32 \rightarrow 16(\rightarrow |\mathcal{Y}|) \rightarrow 32 \rightarrow 64 \rightarrow d]$ , where  $d$  and  $|\mathcal{Y}|$  are data dependent and  $K$  varies between  $[10, 20, 30, 40, 50]$ . Each hidden layer uses the *leakyReLU* activation function and *dropout* regularization with a dropout rate of 0.2. We implemented the FsNet in *keras* and used the *RMSprop* optimizer with a split of 50 : 50 samples in train and test sets for all experiments. Because the number of samples was limited, we performed the experiments upto 6400 epochs with a learning rate of  $\eta = 10^{-3}$ , initial temperature  $\tau_0 = 10$ , and end temperature  $\tau_E = 0.01$  in the annealing schedule. We used six high-dimensional standard datasets from the biological domain.<sup>1</sup>. Table 1 lists the details of these dataset.

**Baseline:** We compared our approach with the CAE [15], a neural network-based unsupervised feature selection method, and the support vector machine with radial basis function kernel (SVM-RBF) owing to their good classification performance on high-dimensional biological data. Because the CAE is an unsupervised method, to provide a fair comparison, we added a softmax layer in the loss function of the CAE, which is referred to as supervised CAE henceforth. The performance was evaluated on four parameters, namely, classification accuracy, reconstruction error, mutual information between the selected features, and model size.

Figure 2 presents a comparison between the training and test behaviors of the proposed FsNet and existing supervised

---

<sup>1</sup>Publicly available at <http://featureselection.asu.edu/datasets.php>

Table 1: Details of Datasets Used

Name	Classes	Size	Dim.
ALLAML [26]	2	72	7,129
CLL.SUB [27]	3	111	11,340
GLI.85 [28]	2	85	22,283
GLIOMA [29]	4	50	4,434
Prostate_GE [30]	2	102	5,966
SMK.CAN [31]	2	187	19,993

CAE methods for  $b = 10$  and  $K = 10$ . The results across the datasets show that the FsNet can learn better than the supervised CAE owing to the reduced number of parameters. Additionally, the correlation between the test and train accuracies of the FsNet model demonstrates its generalization capability in comparison to the supervised CAE, which seems to be overfitted under such high dimensional data and limited number of samples. Table 2 presents the test accuracy for the proposed FsNet and supervised CAE at various numbers of features selected on the six datasets. The experiments show that the FsNet performs consistently better than the supervised CAE; however, there is a slight decrease in the test accuracy when the number of features  $K$  is increased because it also increase the number of parameters in the network, thereby reducing the generalization capability of the model. The comparison of the test reconstruction error for the FsNet and supervised CAE is shown in Figure 3. The FsNet achieves better or competitive reconstruction error than the supervised CAE across the datasets. This shows that the features selected by the FsNet not only have high correlation with the target variable but also are better representatives of all the features in the dataset.

Furthermore, minimum redundancy is another criteria to measure the validity of the selected features. According to this criteria, the selected features should have minimum dependencies between themselves. Mutual information is widely used to measure the dependency between two random variables  $X$  and  $Y$  as

$$I(X, Y) = \sum_{\mathbf{x} \in \mathbf{X}} \sum_{\mathbf{y} \in \mathbf{Y}} p_{XY}(\mathbf{x}, \mathbf{y}) \log \left( \frac{p_{XY}(\mathbf{x}, \mathbf{y})}{p_X(\mathbf{x})p_Y(\mathbf{y})} \right), \quad (9)$$

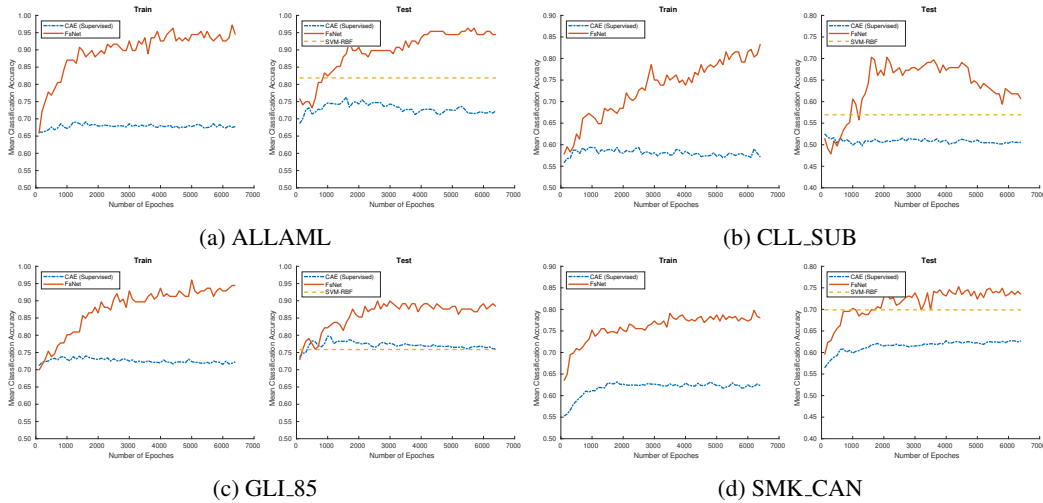


Figure 2: Comparison between the proposed FsNet and existing supervised CAE approaches for training and test accuracy over the epochs.

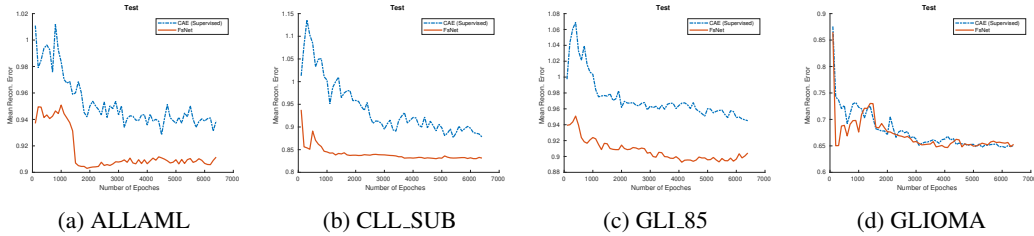


Figure 3: Comparison between the proposed FsNet and existing supervised CAE approaches for test reconstruction error over the epochs.

Table 2: Comparison of the test accuracy for the FsNet and supervised CAE at various number of features selected.

Dataset	K →	10		20		30		40		50	
		acc	epoch								
ALLAML	FsNet	<b>0.9444</b>	5000	0.6944	2000	<b>0.8333</b>	6000	<b>0.7500</b>	1000	<b>0.7593</b>	2000
	CAE	0.7458	1000	<b>0.7458</b>	1000	0.7458	1000	0.7458	1000	0.7458	1000
CLL.SUB	FsNet	<b>0.6788</b>	3000	<b>0.5273</b>	2000	<b>0.6061</b>	4000	<b>0.6364</b>	5000	<b>0.5818</b>	3000
	CAE	0.5127	3000	0.5127	3000	0.5127	3000	0.5127	3000	0.5127	3000
GLL85	FsNet	<b>0.8992</b>	3000	<b>0.8140</b>	4000	0.7364	3000	0.7209	5000	<b>0.8372</b>	4000
	CAE	0.7977	1000	0.7977	1000	<b>0.7977</b>	1000	<b>0.7977</b>	1000	0.7977	1000
GLIOMA	FsNet	<b>0.6533</b>	6000	<b>0.5733</b>	6000	<b>0.6133</b>	5000	<b>0.5733</b>	2000	<b>0.5867</b>	5000
	CAE	0.5260	1000	0.5280	3000	0.5280	3000	0.5280	3000	0.5260	1000
Prostate_GE	FsNet	<b>0.9150</b>	2000	0.6863	1000	<b>0.8301</b>	2000	<b>0.7843</b>	6000	<b>0.8301</b>	3000
	CAE	0.7618	1000	<b>0.7618</b>	1000	0.7618	1000	0.7618	1000	0.7618	1000
SMK_CAN	FsNet	<b>0.7384</b>	3000	<b>0.6774</b>	1000	0.6523	1000	<b>0.6523</b>	5000	<b>0.6452</b>	3000
	CAE	0.6274	4000	0.6274	4000	<b>0.5984</b>	1000	0.6274	4000	0.6274	4000

where  $p_{XY}(\mathbf{x}, \mathbf{y})$  is the joint density, and  $p_X(\mathbf{x})$  and  $p_Y(\mathbf{y})$  are the marginal probabilities of  $p_{XY}(\mathbf{x}, \mathbf{y})$ , respectively. We used the average mutual information between all pairs of the selected features to compare the validity of the features selected by the FsNet and CAE. The average mutual information is defined as

$$\hat{I}(\mathcal{S}) = \frac{2}{K(K-1)} \sum_{i,j \in \mathcal{S}, j > i} I(\mathbf{u}_i, \mathbf{u}_j). \quad (10)$$

As evident from Figure 4, the average mutual information between the features selected by the FsNet is significantly less than that selected by the CAE across all datasets. This shows that the FsNet selects the features with minimum redundancy in comparison to the CAE owing to the use of *dual softmax* and *unique\_argmax* functions in the selector layer where the former attempts to reduce the redundancy, while the latter avoids duplicate feature selection.

Table 3 lists the model sizes<sup>2</sup> in kilobytes (KBs) for the FsNet and supervised CAE. The results show that the FsNet reduces the model size significantly depending on the number of features being selected ( $K$ ) and the size of feature embedding ( $b$ ). The FsNet compresses the model size by 25–157 folds in comparison to the supervised CAE. This reduction in model size is due to the use of the tiny networks for predicting the weight of the fat selector and reconstruction layers. The number of parameter in the selector layer of the supervised CAE are  $O(dK)$ , while in FsNet, the weight predictor network of the selector layer has  $O(bK)$  parameters. Similarly, the number of parameters in the reconstruction layer of the supervised CAE is  $O(dh')$ , while in FsNet, the weight predictor network of the reconstruction layer has  $O(bh')$  parameters.

<sup>2</sup>Model size figures are the size as the *keras* model on the disk.

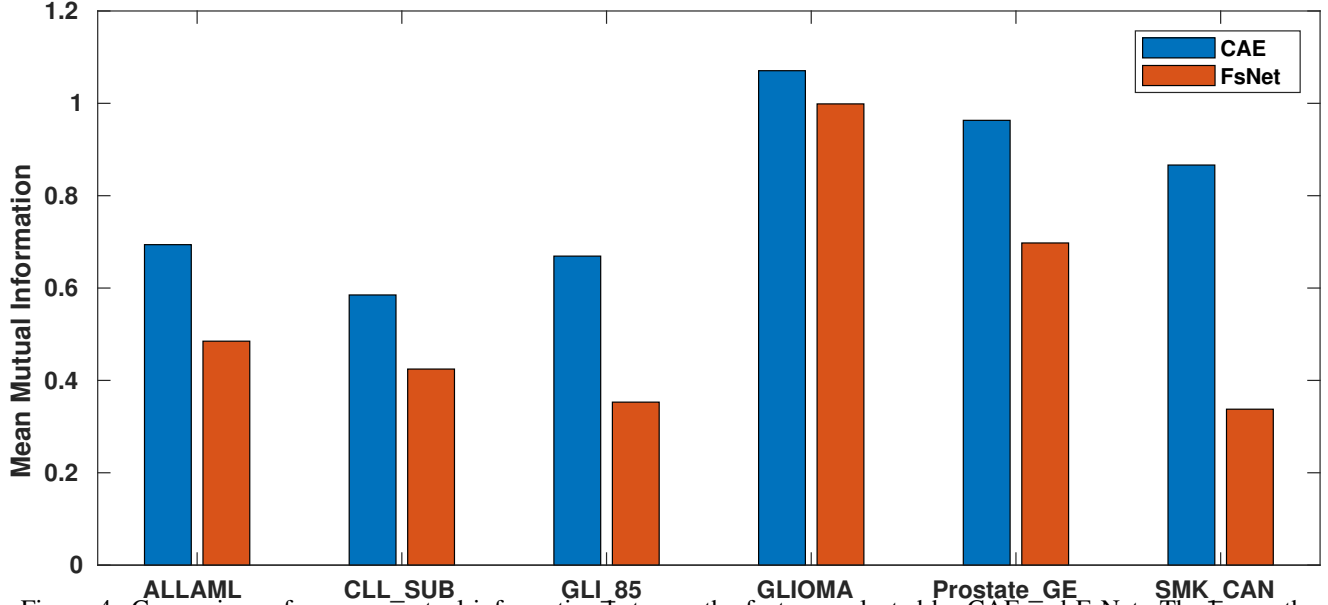


Figure 4: Comparison of average mutual information between the features selected by CAE and FsNet. The lower, the better.

Table 3: Comparison of the supervised CAE and FsNet for the model size<sup>2</sup> (KBs) at various numbers of features selected.

Dataset	K →	10	20	30	40	50
ALLAML	CAE	4280	4844	5404	5968	6528
	FsNet	108 (40×)	116 (42×)	120 (45×)	128 (47×)	132 (49×)
CLL.SUB	CAE	6748	7640	8532	9420	10312
	FsNet	108 (62×)	116 (66×)	120 (71×)	128 (74×)	132 (78×)
GLI.85	CAE	13160	14908	16652	18400	20144
	FsNet	108(122×)	116 (129×)	120 (139×)	128 (144×)	132 (153×)
GLIOMA	CAE	2704	3056	3404	3756	4108
	FsNet	108 (25×)	116 (26×)	120 (28×)	128 (29×)	132 (31×)
Prostate_GE	CAE	3600	4072	4544	5012	5484
	FsNet	108 (33×)	116 (35×)	120 (38×)	128 (39×)	132 (42×)
SMK.CAN	CAE	11820	13388	14952	16520	18088
	FsNet	108 (109×)	116 (115×)	120 (125×)	128 (129×)	132 (137×)

The model compression ratio (CR) for the FsNet w.r.t supervised CAE is

$$CR = \frac{|\theta_s| + |\theta_r| + s}{|\omega_s| + |\omega_r| + s} = \frac{dh + h'd + s}{bh + h'b + s} = O\left(\frac{d}{b}\right), \quad (11)$$

where  $s = |\theta_e| + |\theta| + |\theta_d|$  is the number of parameters in rest of the network. Thus, FsNet has  $\approx \frac{d}{b}$  times less parameters in comparison to supervised CAE.

## 5 Conclusion

The proposed approach can select unique features with minimum redundancy, maximum relevance with the class scores, and minimal feature reconstruction error. Minimum redundancy was achieved owing to the use of the horizontal and vertical softmax layers for the distribution of weight values of a feature in the weight prediction network and the concrete

random variable in the selector layer, respectively. The use of tiny weights for the fat matrices not only reduced the number of parameters but also stabilized the model and made it suitable for training with a limited number of samples. The experiments on several biological datasets demonstrated the robustness of the proposed FsNet for high-dimensional feature selection under a limited number of samples.

## References

- [1] Yixue Li and Luonan Chen. Big biological data: Challenges and opportunities. *Genomics, Proteomics & Bioinformatics*, 12(5):187–189, 2014.
- [2] Vivien Marx. The big challenges of big data. *Nature*, 498(7453), 2013.
- [3] Xiucui Ye, Hongmin Li, Akira Imakura, and Tetsuya Sakurai. Distributed collaborative feature selection based on intermediate representation. In *IJCAI*, 2019.
- [4] Di Ming and Chris Ding. Robust flexible feature selection via exclusive L21 regularization. In *IJCAI*, 2019.
- [5] Shuangli Liao, Quanyue Gao, Feiping Nie, Yang Liu, and Xiangdong Zhang. Worst-case discriminative feature selection. In *IJCAI*, 2019.
- [6] Makoto Yamada, Wittawat Jitkrittum, Leonid Sigal, Eric P Xing, and Masashi Sugiyama. High-dimensional feature selection by feature-wise kernelized lasso. *Neural computation*, 26(1):185–207, 2014.
- [7] Makoto Yamada, Jiliang Tang, et al. Ultra high-dimensional nonlinear feature selection for big biological data. *IEEE TKDE*, 30(7):1352–1365, 2018.
- [8] Hector Climente-Gonzalez, Chlo-Agathe Azencott, Samuel Kaski, and Makoto Yamada. Block HSIC Lasso: model-free biomarker detection for ultra-high dimensional data. *Bioinformatics*, 35(14):i427–i435, 07 2019.
- [9] Robert Tibshirani. Regression shrinkage and selection via the lasso. *J. Royal Stat. Society*, 58(1):267–288, 1996.
- [10] Mahdokht Masaeli, Glenn Fung, and Jennifer G. Dy. From transformation-based dimensionality reduction to feature selection. In *ICML*, 2010.
- [11] Makoto Yamada, Yuta Umezumi, Kenji Fukumizu, and Ichiro Takeuchi. Post selection inference with kernels. In *AISTATS*, 2018.
- [12] Pascal Vincent, Hugo Larochelle, et al. Stacked denoising autoencoders: Learning useful representations in a deep network with a local denoising criterion. *JMLR*, 11:3371–3408, 2010.
- [13] Piotr Iwo Wójcik and Marcin Kurdziel. Training neural networks on high-dimensional data using random projection. *PAA*, 22(3):1221–31, 2019.
- [14] G. E. Dahl, J. W. Stokes, Li Deng, and Dong Yu. Large-scale malware classification using random projections and neural networks. In *ICASSP*, 2013.
- [15] Muhammed Fatih Balin, Abubakar Abid, and James Y. Zou. Concrete autoencoders: Differentiable feature selection and reconstruction. In *ICML*, 2019.
- [16] C. J. Maddison, Andriy Mnih, and Yee Whye Teh. The concrete distribution: A continuous relaxation of discrete random variables. In *ICLR*, 2017.
- [17] Ron Kohavi and George H. John. Wrappers for feature subset selection. *Artif. Intell.*, 97(1-2):273–324, 1997.

- [18] Antanas Verikas and Marija Bacauskiene. Feature selection with neural networks. *Pattern Recognition Letters*, 23(11):1323–1335, 2002.
- [19] Debaditya Roy, K. Sri Rama Murty, and C. Krishna Mohan. Feature selection using deep neural networks. In *IJCNN*, 2015.
- [20] Vadim Borisov, Johannes Haug, and Gjergji Kasneci. Cancelout: A layer for feature selection in deep neural networks. In *ICANN*, 2019.
- [21] Qian Wang, Jiaying Zhang, Sen Song, and Zheng Zhang. Attentional neural network: Feature selection using cognitive feedback. In *NIPS*, 2014.
- [22] Yang Young Lu, Yingying Fan, Jinchi Lv, and William Stafford Noble. DeepPINK: reproducible feature selection in deep neural networks. In *NeurIPS*, 2018.
- [23] Wenlin Chen, James T. Wilson, Stephen Tyree, Kilian Q. Weinberger, and Yixin Chen. Compressing neural networks with the hashing trick. In *ICML*, 2015.
- [24] Adriana Romero, Pierre Luc Carrier, et al. Diet networks: Thin parameters for fat genomics. In *ICLR*, 2017.
- [25] Bo Liu, Ying Wei, Yu Zhang, and Qiang Yang. Deep neural networks for high dimension, low sample size data. In *IJCAI*, 2017.
- [26] TR Golub, DK Slonim, et al. Molecular classification of cancer: class discovery and class prediction by gene expression monitoring. *Science*, 286(5439):531–7, 1999.
- [27] C. Haslinger, N. Schweifer, et al. Microarray gene expression profiling of b-cell chronic lymphocytic leukemia subgroups defined by genomic aberrations and vh mutation status. *J Clin Oncol*, 22(19):3937–3949, 2004.
- [28] W. A. Freije, F. E. Castro-Vargas, et al. Gene expression profiling of gliomas strongly predicts survival. *Cancer Res*, 64(18):6503–6510, 2004.
- [29] C. L. Nutt, D. R. Mani, R. A. Betensky, et al. Gene expression-based classification of malignant gliomas correlates better with survival than histological classification. *Cancer Res.*, 63:1602–1607, 2003.
- [30] D. Singh, P. Febbo, K. Ross, et al. Gene expression correlates of clinical prostate cancer behavior. *Cancer Cell*, pages 203–209, 2002.
- [31] A. Spira, J. E. Beane, et al. Airway epithelial gene expression in the diagnostic evaluation of smokers with suspect lung cancer. *Nat Med*, 13(3):361–366, 2007.